Investigation on the thermal effects during nanometric cutting process while using nanoscale diamond tools

Zhen Tong[1,2], Yingchun Liang[2], Xuechun Yang[3], and Xichun Luo[1*,3]

1 Department of Design, Manufacture & Engineering Management, University of Strathclyde, Glasgow G1 1XQ, UK

2 Center for Precision Engineering, Harbin Institute of Technology, Harbin 150001, China

3 Innovative Centre for Unit-based Logistics Engineering & Technology, Hefei University, Hefei 230601, China

*Email: xichun.luo@strath.ac.uk

Tel: 0141 574 5280   Fax: 0141 552 7986

Abstract

In this paper, large scale molecular dynamics simulations are carried out to investigate the thermal effect on nanometric cutting of copper while using a single tip and a multi-tip nanoscale diamond tool. A new concept of atomistic equivalent temperature is proposed and used to characterize the temperature distribution in the cutting zone. The results show that the cutting heat generated while using a multi-tip tool is larger than that of using a single tip tool. The local temperature is found to be higher at the inner sides of the multi-tip tool cutting edges than the outer sides. Applying centro-symmetry parameters and radius distribution function, the local annealing process and its effect on the integrity of the machined nanostructures are analyzed. It is observed that the local annealing at the machined surface can improve the surface integrity of the machined nanostructures, especially in the multi-tip diamond tool cutting process. There exists a great potential to control the thickness of residual atomic defect layer through an optimal selection of the cutting speed with designed depth of cut.

(Some figures in this article are in colour only in the electronic version)

Keywords: Molecular dynamics; Thermal effect; Nanometric cutting; Multi-tip tool; Nanostructure

1. Introduction

In recent decades, numerous nanofabrication techniques such as optical and electron beam lithography, focused ion beam (FIB) milling, nanoimprinting, femtosecond laser machining etc. have been developed to fabricate nanostructures. These nanostructures are the building blocks for many emerging high-tech products such as plasmonic lens, bio-sensors, solar cell, and high density magnetic hard disk etc [1-3]. However, due to the inherent limitations of these fabrication techniques, particularly the inability for scale-up manufacturing of high quality nanodevices, these methods fail to meet the increasing demand in commercializing functional nanostructured devices.

Diamond turning using multi-tip diamond tools has recently been proven to be a promising method for scale-up manufacturing of micro/nano structures on work material surfaces [2, 4-7]. Through ultra precision scratching/turning operations, it is possible to replicate micro/nano structures pre-featured on the tip of a diamond tool onto a target specimen with high formation accuracy. Periodic micro grooves [4-5], arrays [6], and diffraction gratings [7] have been successfully obtained by several research groups by using multi-tip tools fabricated by FIB (with tool tip dimensions ranging from 15 μm to 100 μm). Recently even nano-gratings with pitch of hundreds of nanometers can be generated by this technique while using nanoscale mult-tip diamond tools (with tool tip width of 150 nm) [2].

However, the formation mechanism of theses nanostructures and the influence factors on form accuracy and surface integrity remain unclear. Obtaining nanostructures with great repeatability is still a challenging task when applying this technique. The cutting heat has long been regarded as a significant factor in nanometric cutting process [3, 8]. It will not only accelerate tool wear, but also significantly influence the material removal, elastic/plastic deformation and local thermal annealing. A detailed investigation into the thermal effects is therefore, crucial to gain great controllability and repeatability in the nanometric cutting process.

Molecular dynamics (MD) simulations have been effectively used to address some fundamental issues related to nanometric cutting processes [3, 8-12]. Atomistic models have been applied to emulate the material removal process during nanometric cutting of copper. Ye et al. [3] and Pei et al. [8, 9] built single tip cutting tool models to investigate the material removal mechanism and the cutting heat performed at different cutting speeds. Fang et al. [10], Kim et al. [11] and Yan et al. [12] have used the pin-tool MD model to study the AFM-based nano-scratching processes. Moreover, the role of friction and tool wear in nanometric machining of copper using single tip tool has also been reported [3, 11, 13]. These studies have made significant contributions towards the understanding of the mechanism of diamond turning of copper. However, no experiments or theoretical models have been developed, for nanometric cutting, to study the thermal effect on nanostructure fabrication process while using nanoscale multi-tip diamond tools.
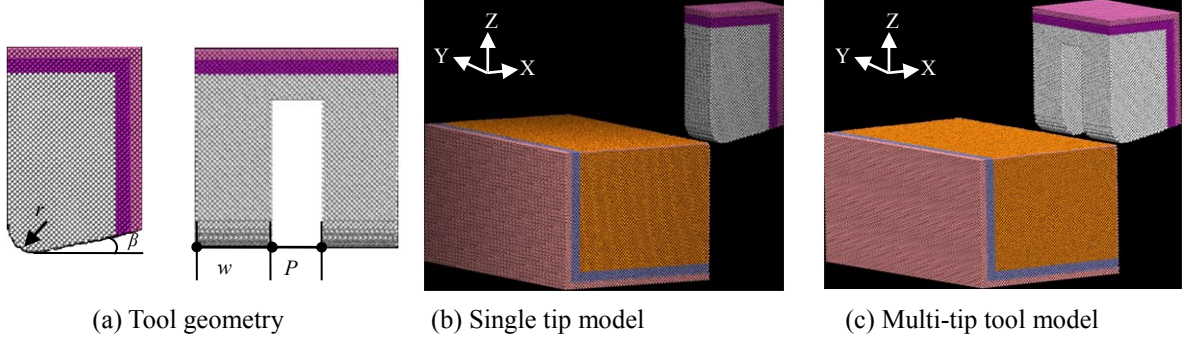
In this paper, atomistic nanometric cutting models are built and conducted to study the thermal effects during the nanometric cutting of copper. In order to benchmark the unique characteristics while using a multi-tip tool, a detailed comparison between the single tip and multi-tip tool cuttings have been carried out in terms of temperature distribution and the integrity of the machined surface.

2. Computational method and the modeling parameters

2.1 Geometric models

To avoid the size effect caused by the period boundary condition [9], large scale nanometric cutting models with free boundary condition in all directions were built for single tip as well as for multi-tip tool cuttings (as shown in figure 1). The geometry of the multi-tip cutting tools is shown in figure 1 (a). The tool-tip width is $15a$ (a = 3.567 Å) with the tool rake angle α being 0º and the tool clearance angle β being 12º. To save computational time, a double-tip diamond tool with a pitch of $10a$ was employed to represent a multi-tip tool. All of the tools were built as deformable bodies with round cutting edges (edge radius of $5a$). Copper is chosen

as workpiece because of its high machinability for diamond turning, particularly suitable for fabrication of

precision drums used in roll-to-roll manufacturing [5]. The workpiece model has a dimension of

$50a_0 \times 80a_0 \times 40a_0$ (a_0 = 3.615 Å). The three orientations of the workpiece are [1 0 0], [0 1 0], and [0 0 1] in the

X, Y, and Z directions, respectively.

(a) Tool geometry   (b) Single tip model   (c) Multi-tip tool model

Figure 1. Models of MD for nanometric cutting simulation

2.2 Potential functions

There are three types of atomic interactions in the MD simulation. For the Cu–Cu interaction the embedded

atom method (EAM) potential proposed by Foiles et al. [14] was used since it has been successfully used in

description of metal materials [3, 9, 15]. The total energy E of the atomistic system comprises summation over

the atomistic aggregate of the individual embedding energy F_i of atom i and pair potential ϕ_{ij} between atom i

and its neighboring atom j, as shown in the following equation:

$$E = \sum_{i} F^i(\sum_{j \neq i}^{n} \rho^i(r^{ij})) + \frac{1}{2} \sum_{ij, i \neq j} \phi_{ij}(r^{ij}) \tag{1}$$

where the lower case Latin superscripts i and j refer to different atoms, r^{ij} is the distance between the atoms i

and j, and $\rho^i(r^{ij})$ is the electron density of the atom i contributed by atom j.

For C-C atoms, we adopted Tersoff potential [16] and computed as follows:

$$V_{ij} = f_C(r_{ij})[f_R(r_{ij}) + b_{ij}f_A(r_{ij})] \tag{2}$$

$$f_C(r) = \begin{cases} 1 : r < R - D \\ \dfrac{1}{2} - \dfrac{1}{2}\sin(\dfrac{\pi}{2}\dfrac{r-R}{D}) : R - D < r < R + D \\ 0 : r > R + D \end{cases} \tag{3}$$

$$f_R(r) = A\exp(-\lambda_1 r) \tag{4}$$

$$f_A(r) = -B\exp(-\lambda_2 r) \tag{5}$$

$$b_{ij} = (1 + \beta^n \zeta_{ij}{}^n)^{-\frac{1}{2n}} \tag{6}$$

$$\zeta_{ij} = \sum_{k \neq i,j} f_C(r_{ik}) g(\theta_{ijk}) \exp[\lambda_3{}^3(r_{ij} - r_{ik})^m] \tag{7}$$

$$g(\theta_{ijk}) = r_{ijk}(1 + \dfrac{c^2}{d^2} - \dfrac{c^2}{[d^2 + (\cos\theta - \cos\theta_0)^2]}) \tag{8}$$

where V_{ij} is the bond energy of all the atomic bonds, i, j, and k label the atoms of the system, r_{ij} is the length of the

ij bond, b_{ij} is the bond order term, θ_{ijk} is the bond angle between the bonds ij and ik, f_R is a two-body term and f_A

includes the three-body interactions. f_C merely represents a smooth cutoff function to limit the range of the

potential, and ζ_{ij} counts the number of other bonds to atom i besides the ij bond.

Morse potential function was selected to describe the interaction between Cu-C, which has been widely used in

MD simulations of nanometric cutting of Cu [12]. A cohesion energy D of 0.087eV, elastic modulus α of 5.14

Å^{-1}, and r_0 of 2.05 Å are specified in present study.
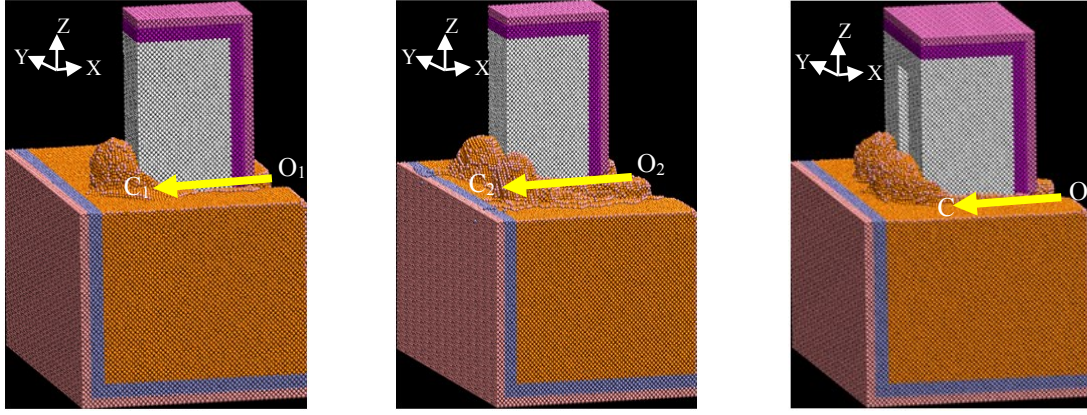
2.3 MD simulation

MD simulations were implemented by using an open source code—LAMMPS [17] compiled on a high

performance computing (HPC) clusters using 24 cores. Before cutting, 85,000 computing time steps were

carried out to freely relax the system to 293 K. During cutting and the thermal annealing processes, the systems

were controlled by NVE ensemble and the thermostat atoms were keeping at a constant temperature of 293 K

through using the velocity scaling method to perform the heat dissipation [8, 12]. The other computational

parameters used in the MD simulations were summarized in table 1 for reference.

Table 1. Workpiece and simulation parameters

	Single tip with multi-pass	Multi-tip with single pass
Workpiece materials	Copper	Copper
Workpiece dimensions	$50a_0 \times 80a_0 \times 40a_0$ ($a_0 = 3.615$ Å)	$50a_0 \times 80a_0 \times 40a_0$ ($a_0 = 3.615$ Å)
Number of atoms	760, 355	894, 870
Time step	1 fs	1 fs
Initial temperature	293 K	293 K
Depth of cut	1 nm	1 nm
Cutting speed	200 m/s	100 m/s, 150 m/s, 200 m/s, 300 m/s

Figure 2 shows the simulation procedure of the nanometric cutting and the traces of the tool. The cutting tools

were applied along the [-1 0 0] direction on the (0 0 1) surface of the copper workpiece. Single tip tool

scratched the work surface along the line O_1C_1 for the first cutting pass (as shown in figure 2 (a)). Then the tool

was moved to point O_2 to scratch again to produce the second nano-groove along the line O_2C_2 with same depth

of cut (as shown in figure 2 (b)). For multi-tip tool cutting, only a single pass was taken along line OC with the

same cutting distance as shown in figure 2(c). In this case, two nano-grooves were formed at the same time by

a single pass. In order to fully reveal the local thermal elastic/plastic recovery of materials during the

nanostructure generation processes, after the cutting, all of the models were allowed to relax for 50,000 time

steps (50 ps) by holding the tool in the fixed loaded position.

| (a) Single tip cutting (1st pass) | (b) Single tip cutting (2nd pass) | (c) Multi-tip cutting with single pass |

Figure 2. Schematic of the nanometric cutting traces
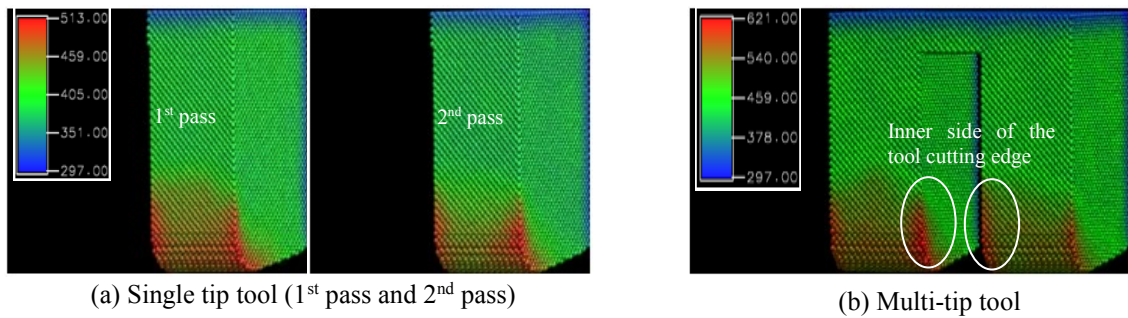
3.   Results and discussion

3.1 Temperature distribution

Cutting heat has been regarded as one of the key factors to influence the quality of the generated nanostructures as well as the tool life in nanometric cutting process. According to the law of equipartition of energy, the representative temperature of a group of atoms can be calculated from the total atomic kinetic energies of the group. A new concept of atomistic equivalent temperature T_i, which is calculated from the statistical average temperature of neighbour atoms around the atom i, is proposed in order to more accurately characterize the variation of temperature during the nanomectric cutting process. As the nature of the temperature is statistical, the accuracy of the temperature calculated significantly depends on the cutoff distance used. In general, the larger the cutoff distance, the lower the calculated temperature. In this paper, a critical radius $r_0 = 4a_0$ was employed to select the neighbour atoms in order to reflect the thermal feature of the short-range structure of copper lattice during nanometric cutting processes. The translation between the atomic kinetic energy and the statistical temperature are computed using the following equation:

$$\frac{1}{2}\sum_{j=1}^{n}m_j v_j^2 = \frac{3}{2}nk_B T_i \tag{9}$$

where n is the number of atoms within the radius r_0, m_j and v_j represent the mass and instantaneous velocity respectively, and k_B is the Boltzmann constant.

The calculated results showed that at initial cutting state the cutting temperature rapidly increased until it reached a stable value at a cutting distance of 15 nm. Figure 3 shows the detailed temperature distributions of the single tip and multi-tip cutting tools at a cutting distance of 17 nm. Atoms are coloured according to their atomistic equivalent temperature. For all the tool models presented here, the highest temperatures were found at the tool cutting edges. For the single tip tool cutting, the atoms with equivalent temperature around 510 K were distributed uniformly around both sides of the tool cutting edges; while for the multi-tip tool cutting, a local temperature of 610 K was found at the inner sides of the tool tips which is higher than other sides. Unlike the single tip tool nanometric cutting where the nano-grooves were generated separately, the two nano-grooves were formed at the same time during multi-tip tool cutting. This will result in a large compression between the inner sides of the tool tips and the workpiece, and thus leading to a high local temperature. Since the high cutting heat is very closely associated with the tool wear, the result indicates that the inner sides' cutting edges of a multi-tip tool are more likely to wear prior to other cutting edges.

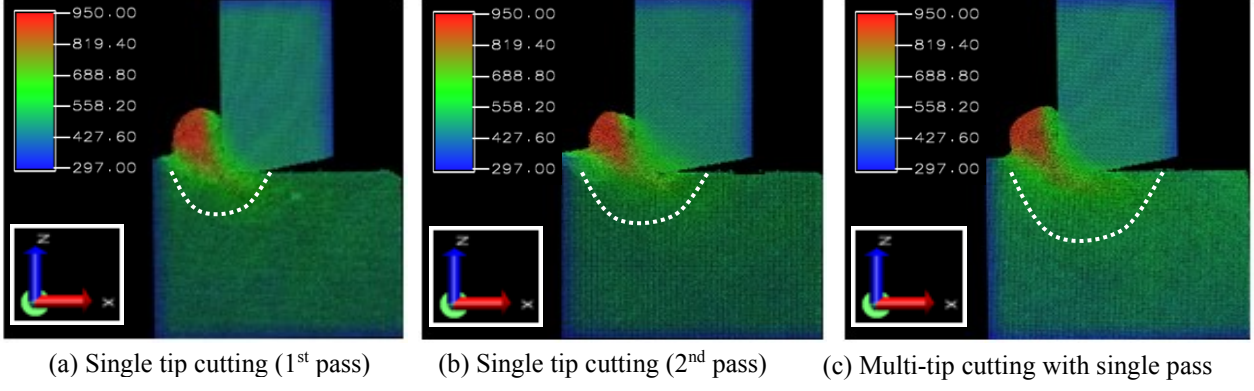(a) Single tip tool (1st pass and 2nd pass)   (b) Multi-tip tool

Figure 3. The temperature distribution of tool tips at a cutting distance of 17 nm.

Figure 4 shows the cross-sectional view of the atomistic equivalent temperature distribution for the single tip tool and the multi-tip tool cuttings. For better visualization, the white dotted lines are used as the boundaries between the low and high temperature zones (> 550K). It is observed that in all simulations, the temperature in
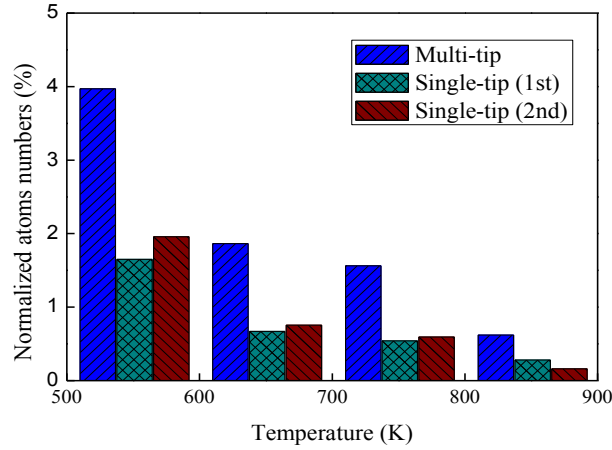
shear zone is around 650 K, but the highest temperature found in the cutting chips is about 900 K. Unlike traditional metal cutting in this study the diamond tool material is significantly harder than the workpiece material i.e. copper. It is a common knowledge that when the cutting tool material is significantly harder than the substrate, the plastic deformation of the softer work material will be the main heat source [18]. In our MD model, the energy transfer between copper and diamond is described by the selected potential functions. At the interface of the diamond tool and copper substrate, there is an atomic layer (with a thickness of several atoms) to transmit the energy between C and Cu atoms. Copper and the diamond materials both have high thermal conductivity. However, the thermal conductivity of the natural diamond was measured to be about 22 W/(cm·K) which is five times more than copper. As a result, a large temperature gradient towards the cutting tool was observed in figure 4. Moreover, the large diamond cutting tool model built in present study also help to release the cutting heat at tool cutting edge. Therefore, the diamond cutting tool would have lower temperature than the copper substrate. The highest cutting temperature was found in the cutting chips.

Nevertheless, it can be seen that the range of high temperature region (> 550 K) when using the multi-tip tool is apparently larger than that of using the single tip tool. In order to further quantify the difference in cutting heat when different kinds of tool were used, detailed analysis has been done by comparing the number of atoms in different temperature ranges. For a better comparison, only the workpiece atoms within the cutting zone (z coordination larger than $20a_0$) were taken into account and the numbers of atoms in different temperature ranges were normalized by the total number of atoms selected (as shown in figure 5). It was found that the proportion of atoms with atomistic equivalent temperature T_i larger than 500 K in the multi-tip tool case was 8.01%, which was more than twice large than that of the single tip tool cutting (being 3.3%). This result well confirm that the cutting heat generated while using the multi-tip tool was much higher than the cutting heat produced during both the first and the second pass of the single tip tool cutting.

(a) Single tip cutting (1st pass) (b) Single tip cutting (2nd pass) (c) Multi-tip cutting with single pass

Figure 4. The cross-sectional views of the temperature distribution at a depth of cut of 17 nm.

Figure 5. The proportion of atoms numbers in different temperature ranges.
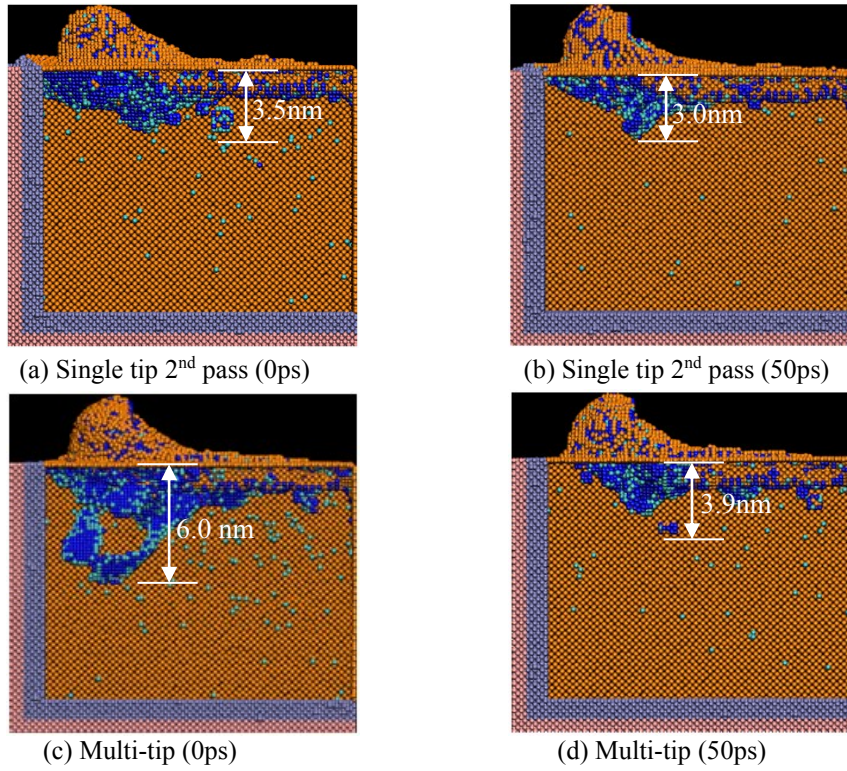
3.2 Thermal annealing at machined surface

It has been widely accepted that re-crystallization happens during local annealing process, not only in ductile

metallic materials [3] but also in brittle materials such as silicon [19] and diamond [20]. In macro machining

practice, after the tool has left the machined region, there is a macroscopic time (~ms) for the machined surface

to relax [3]. And by that time, atomic defects and dislocations under the subsurface might be able to get

annealed partly. In nanometric cutting, the thermal effects happen in such a short timescale. To accurately

detect and measure the temperature distribution, it requires a thermal measurement system with extremely short

response time and high resolution. However, the spectral wavelength of sensors used in most current

commercial infra-red thermography are ranging from 0.8 μm to 14 μm with the response time ranging from 2

ms to 120 ms. It is therefore very difficult to detect and monitor the cutting heat accurately by current

temperature measurement systems. On the other hand, MD simulation provides an effective way to solve this problem by allowing the atomistic insight into the material thermal behavior during nanaometric cutting processes.

In present work, in order to well simulate the relaxation process and investigate the thermal effects when different kinds of tools were used, time relaxations of the machined work material were performed for both the single tip and multi-tip tool cuttings. It has been found through trial simulations that a period of 50 ps relaxation process was enough for the present system to cool down to 293 K. For the identification of the damages formed during the cutting process, centro-symmetry parameter (CSP) was employed as it is less sensitive to the temperature increase compared with other methods such as atomic coordinate number and the slip vector [9]. Moreover, radial distribution function (RDF) [21] was further employed to identify the changes in the lattice structure during the relaxation process.

Figure 6 shows the cross-sectional views of the defect zones at 0 ps and 50 ps. For better comparison, only the atoms in the defect zone were selected for analysis and the atoms in the defect-free zone were removed from the visualizations [22]. It can be seen that before the relaxation, there are large number of dislocations and atomic defects beneath the tool tip (figure 6(a) and (c)). The depth of the subsurface atomic defect layer in the multi-tip tool cutting is about ~ 6 nm which is nearly twice of the single tip tool cutting (being ~ 3.5 nm). However, as shown in figure 6 (b), most of atomic defects and dislocations in the machined area are annealed after 50 ps for the single tip tool cutting. For multi-tip tool cutting, the atomic defects and dislocations are also remarkably annealed after the relaxation process (as shown in figure 6 (d)), leaving behind an almost dislocation-free machined workpiece.
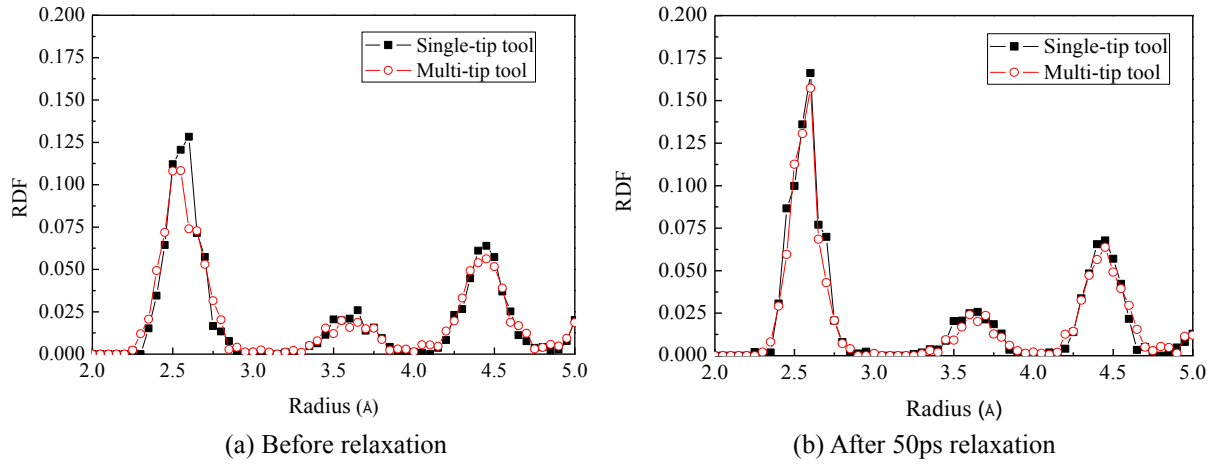
Figure 6. The cross-sectional views of atomic defects distributions at 0 ps and 50ps.
Cyan and blue atoms represent particle dislocation and stacking fault, respectively.

In order to further identify the lattice integrity of the machined structure, the radial distribution functions (RDF) of the machined nanostructures were calculated before and after the relaxation process. As shown in figure 7 (a), before relaxation, the RDF value of the first and the third peak for the nanostructure machined by the multi-tip tool are slightly smaller than those of the nanostructure created by using single tip tool, which indicates that the atoms are in a higher disorder in the case of multi-tip tool cutting; however after the relaxation process, there is an increase of the first peak value of RDF for both the single tip and multi-tip tool cutting, and the two RDF curves have nearly the same shape (as shown in figure 7 (b)). This result is in good agreement with the CSP result and indicates that local re-crystallization takes place on the machined surface.

Nevertheless, it is noted that, the local re-crystallization observed in multi-tip tool cutting is more noticeable than the single tip tool cutting. Although the depth of the atomic defect layer before relaxation when using the multi-tip tool was much larger than that of using the single tip tool, most of the defects were annealed and left

almost an ideal FCC lattice structure after the relaxation process. As evident from figure 6 (b) and (d), the depths of the residual atomic defect layer are 3.0 nm and 3.9 nm for the single tip and multi-tip tool cuttings, respectively. The cutting heat produced during the nanometric cutting process provides the thermal energy for the defects to get annealed [3]. Therefore, the thermal annealing plays a significant role in obtaining high quality nanostructures during the nanometric cutting process, especially when using a multi-tip tool.

(a) Before relaxation   (b) After 50ps relaxation

Figure 7. Radial distribution function (RDF) of machined nanostructures.
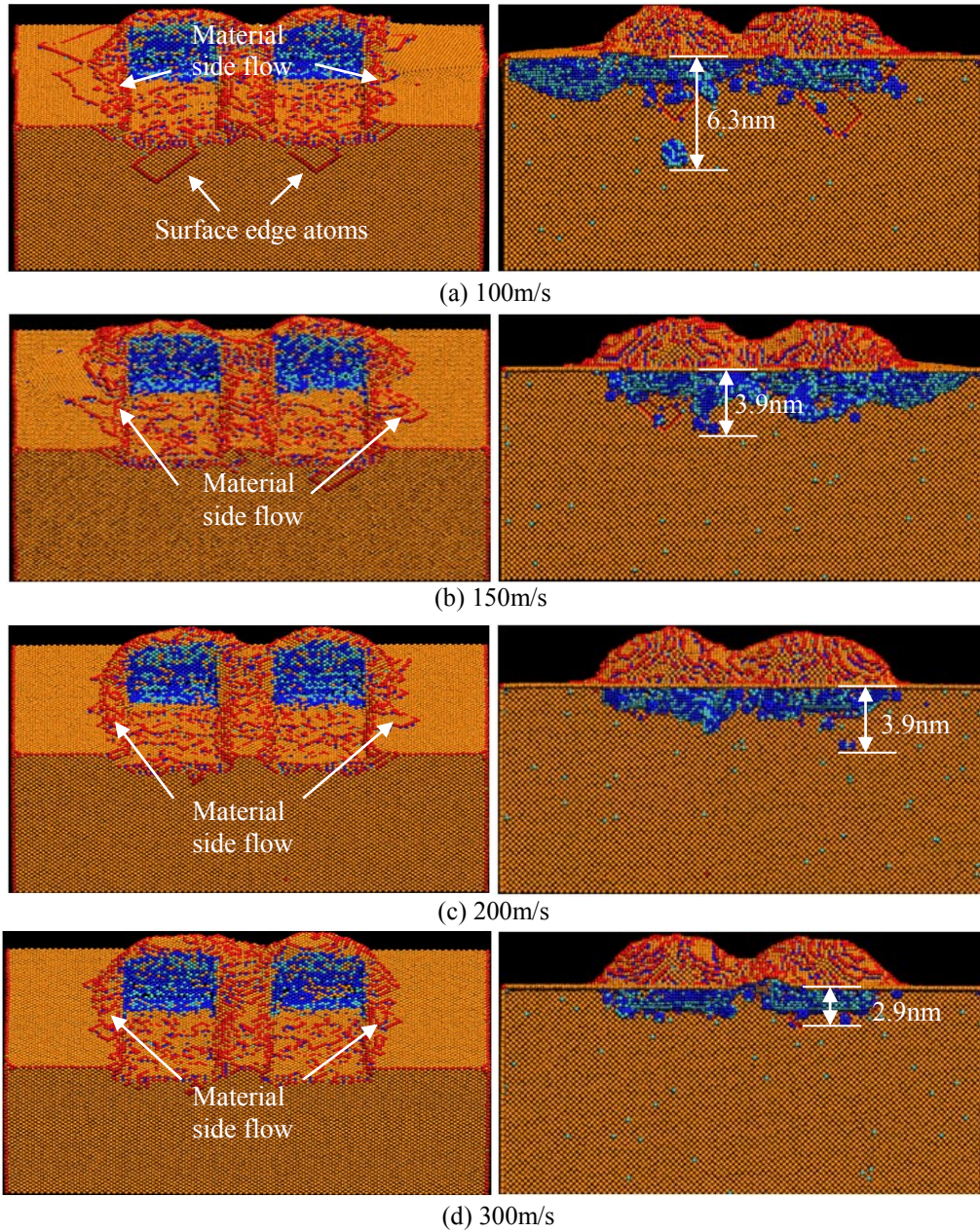
3.3 Effect of cutting speed

In metal cutting process, the cutting zone temperature significantly depends on the cutting speed. In order to investigate the thermal effect under different cutting speeds, simulations of nanometric cutting process by using multi-tip tools were performed over a wide range of cutting speed (100 m/s, 150 m/s, 200 m/s, and 300 m/s) with depth of cut of 1 nm.

The nano-grooves and inside views of atomic defects distribution after 50 ps relaxation are shown in figure 8. For the case of cutting speed being 100 m/s, there were large numbers of surface edge atoms left (red colour) after the relaxation process (figure 8 (a)). Because the surface edge atoms also reflects the slip plan of dislocations inside the workpiece, to some extent, the density and distribution of these edge atoms are able to indicate the range and slip plans of material plastic flow [22]. It is found that with the increase of the cutting

speed, especially when the cutting speed is higher than 200 m/s, the number of surface edge atoms and the range of material side flow are remarkably decreased. The nano-grooves machined by using a cutting speed of 300 m/s has the best surface integrity (as shown in figure 8 (b)-(d)). Moreover, the range and depth of residual atomic defect layer after annealing were found to be significantly decreased with the cutting speed. The depth of residual damaged layer being 2.9 nm under the cutting speed of 300 m/s is much smaller than that of 6.3 nm for the case of the cutting speed at 100 m/s; while the depth of residual damaged layer for the cases of 150 m/s and 200 m/s are the same (being 3.9 nm). Under all the above cutting conditions, no extra thermo-induced damage was found after a cutting distance of 18 nm. The result indicates the great potential to control the thickness of residual atomic defect layer through selection of optimal cutting speed under the adopted depth of cut when using nanoscale multi-tip diamond tools.

To achieve better understanding of the effect of cutting speed on the cutting heat produced during the nanometric cutting process, the proportions of atoms with atomistic temperature that is larger than 400 K are calculated and shown in figure 9. On one hand, the cutting heat increases with the increase of the operational cutting speed. As shown in figure 9 (a), the proportional of atoms at each temperature range increase with the increase the cutting speed. However, the existence of workpiece atoms with the equivalent atomistic temperature that is larger than 600K only appears when the cutting speed is equal or larger than 150 m/s. This important result explains well the variation of surface integrity and the depth of residual subsurface atomic defect layer under different cutting speeds which has been discussed above. When the cutting speed is high enough, the cutting heat generated at the high cutting speed would provide enough thermal energy for annealing the atomic defects and facilitating the nanostructure formation process as the dislocations movement and diffusional creep are more easily to activate at a relatively high temperature [23]. The higher the cutting speed, the higher the local cutting heat generated, and thus the less the numbers of residual atomic defects left.
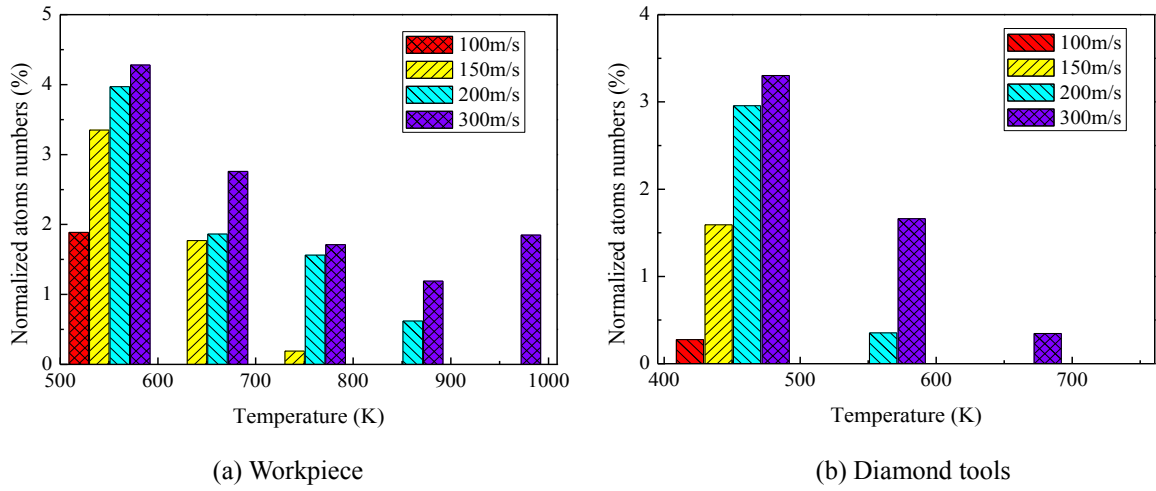
Figure 8. The nano-grooves and inside views of atomic defects distribution after 50ps relaxation. Cyan, blue, and red atoms represent particle dislocation, stacking fault, and surface edge atoms respectively.

On the other hand, the high cutting heat produced at high cutting speed will result in the initialization of the tool wear at the cutting edge and decrease the tool life [24, 25]. Figure 9 (b) shows the proportions of the diamond tool atoms in different temperature ranges. It is found that the tool atoms with the equivalent atomistic temperature that is larger than 500 K only appears when the cutting speed is higher than 150 m/s. Although the high cutting heat produced at high cutting speed would provide enough thermal energy for annealing the atomic defects [3], to some extent, the increase of the cutting heat at the tool cutting edges would in turn soften the

C-C bond strength and accelerate the tool wear [26]. In this sense, a high cutting speed is not preferable due to the early induced tool wear. Moreover, the vibrations and the motional errors induced by the increase of cutting speed would degrade the formation accuracy of the nanostructures and the surface integrity. As a result, it is to be concluded that a balance between the targeted quality of nanostructures and the tool life should be critically considered while choosing the cutting speed for the diamond turning with nanoscale multi-tip tools.

(a) Workpiece   (b) Diamond tools

Figure 9. The proportion of atoms numbers in different temperature ranges under different cutting speeds.

4. Conclusions

The MD simulations presented in this paper reveal the detailed thermal behaviors of work materials and provide a useful theoretical support for determining the cutting speed when perform the nanometric cutting using nanoscale multi-tip diamond tools. The conclusions can be drawn as follows:

(1) The atomistic equivalent temperature provides a new effective way to characterize local temperature distribution during nanometric cutting processes. The highest temperature was found in cutting chips. The cutting heat produced during multi-tip tool cutting is found to be larger than the single tip tool cutting.

(2) The local temperature is found to be higher at the inner sides of the nanoscale multi-tip diamond tool cutting edges than that of the outer sides suggesting that the inner sides' cutting edges are more likely to wear prior to other cutting edges.

(3) Local thermal annealing process takes place on the machined area and plays a major role in obtaining high quality nanostructures. When the cutting heat produced during the cutting process is high enough, most of the subsurface atomic defects are able to get annealed during the relaxation process.

(4) High cutting speed can accelerate thermal annealing process observed at the machined area. A balance between the machining quality of nanostructures and the tool life should be critically considered while choosing the cutting speed for nanometric cutting with nanoscale multi-tip tools.

References

[1] L.B. Kong, C.F. Cheung, X.Q. Jiang, W.B. Lee, S. To, L. Blunt, P. Scott (2010) Characterization of surface generation of optical microstructures using a pattern and feature parametric analysis method. Precis. Eng. 34: 755–766

[2] J. Sun, X. Luo, W. Chang, J. M. Ritchie, J. Chien and A. Lee (2012) Fabrication of periodic nanostructures by single-point diamond turning with focused ion beam built tool tips. J. Micromech. Microeng. 22: 115014

[3] Y Y Ye, R Biswas, J R Morris, A Bastawros and A Chandra (2003) Molecular dynamics simulation of nanoscale machining of copper. Nanotechnol. 14: 390–396

[4] D.P. Adamsa, M. J. Vasile, A.S.M. Krishnan (2000) Microgrooving and microthreading tools for fabricating curvilinear features. Precis. Eng. 24: 347–356

[5] Y.N. Picard, D.P. Adams, M.J. Vasile, M.B. Ritchey (2003) Focused ion beam-shaped microtools for ultra-precision machining of cylindrical components. Precis. Eng. 27 (1): 59–69

[6] X Ding, G C Lim, C K Cheng, David Lee Butler, K C Shaw, K Liu and W S Fong, (2008) Fabrication of a micro-size diamond tool using a focused ion beam. J. Micromech. Microeng. 18: 075017

[7] Z.W. Xu, F.Z. Fang, S. J. Zhang, X. D. Zhang, X. T. Hu, Y. Q. Fu, L. Li (2010) Fabrication of micro DOE using micro tools shaped with focused ion beam. Opt. Expr. 18 (8): 8025–8032

[8] Q.X. Pei, C. Lu, H.P. Lee. (2007) Large scale molecular dynamics study of nanometric machining of copper. Comput. Mater. Sci. 41 (2): 177–185

[9] Q.X. Pei, C. Lu, H.P. Lee, Y.W. Zhang (2009) Study of Materials Deformation in Nanometric Cutting by Large-scale Molecular Dynamics Simulations. Nanoscale Res. Lett. 4: 444–451

[10] T.H. Fang and C.I. Weng (2000) Three-dimensional molecular dynamics analysis of processing using a pin tool on the atomic scale. Nanotechnol. 11: 148–153

[11] M.H. Cho, S.J. Kim, D.S. Lim, H. Jang (2005) Atomic scale stick-slip caused by dislocation nucleation and propagation during scratching of a Cu substrate with a nanoindenter: a molecular dynamics simulation. Wear 259 (7-12): 1392–1399

[12] Yongda Yan, Tao Sun, Shen Dong, Yingchun Liang (2007) Study on effects of the feed on AFM-based nano-scratching process using MD simulation. Comput. Mater. Sci. 40 (1): 1–5

[13] ZC Lin, JC Huang (2008) A study of the estimation method of the cutting force for a conical tool under nanoscale depth of cut by molecular dynamics. Nanotechnology 19: 115701

[14] S. M. Foiles, M. I. Baskes and M. S. Daw (1986) Embedded-atom-method functions fo the fcc metals Cu, Ag, Au, Ni, Pd, Pt, and their alloys. Phys. Rev. B. 33(12): 7983–7991

[15] P. Z. Zhu, Y. Z. Hu, T. B. Ma, and H. Wang (2010) Study of AFM-based nanometric cutting process using molecular dynamics. Appl. Surf. Sci. 256 (23): 7160–7165

[16] J. Tersoff (1988) New empirical approach for the structure and energy of covalent systems. Phys Rev B, Condens Mater. 37 (12): 6991–7000

[17] S. Plimpton (1995) Fast parallel algorithms for short range molecular dynamics. J. Comput. Phys. 117, 1–19

[18] Vahid Norouzifard, Mohsen Hamedi (2014) Experimental determinationofthetool–chip thermalcontact conductance inmachiningprocess. Int. J. Mach. Tool & Manu.,84: 45–57

[19] K. Nordlund and R. S. Averback (1997) Point defect movement and annealing in collision cascades. Phys. Rev. B, 56: 2421–2431

[20] R. Kalish, A. Reznik, S. Prawer, D. Saada, and J. Adler (1999) Ion-Implantation-Induced Defects in Diamond and Their Annealing: Experiment and Simulation. Phys. Stat. Sol. 174: 83–99

[21] <http://isaacs.sourceforge.net/phys/rdfs.html>, g(r) RDF Explanation accessed on 21 Nov. 2011

[22] Z. Tong, Y.C. Liang, X.Q. Jiang, X.C. Luo (2014) An atomistic investigation on the mechanism of machining nanostructures when using single tip and multi-tip diamond tools. Appl. Surf. Sci. 290: 458–465

[23] L. Lu, M.L. Sui, K. Lu (2000) Superplastic Extensibility of Nanocrystalline Copper at Room Temperature. Science 287: 1463-1466

[24] H. Saglam, S. Yaldiz, F. Unsacar (2007) The effect of tool geometry and cutting speed on main cutting force and tool tip temperature. Mater. and Design 28: 101–111

[25] S.J. Kim, D. Le, S.W. Lee, K.H. Song, and D.Y. Lee (2014) Experiment-based statistical prediction on diamond tool wear in micro grooving Ni-P alloys. Diam. & Relat. Mater. 41: 6–13

[26] K. Cheng, X. Luo, R. Ward, and R. Holt (2003) Modeling and simulation of the tool wear in nanometric cutting. Wear 255: 1427–1432